Impact of magnetic storms on the global TEC distribution

Donat V. Blagoveshchensky[1], Olga A. Maltseva[2], Maria A. Sergeeva[3,4]

[1]Saint-Petersburg State University of Aerospace Instrumentation, 67, Bolshaya Morskaya, Saint-Petersburg, 190000, Russia
[2]Institute for Physics, Southern Federal University, Stachki, 194, Rostov-on-Don, 344090, Russia
[3]SCiESMEX, LANCE, Instituto de Geofisica, Unidad Michoacan, Universidad Nacional Autonoma de Mexico, Morelia, 58089, Mexico
[4]CONACYT, Instituto de Geofisica, Unidad Michoacan, Universidad Nacional Autonoma de Mexico, Morelia, 58089, Mexico

Correspondence to: Maria A. Sergeeva (maria.a.sergeeva@gmail.com)

Abstract. The study is focused on the analysis of Total Electron Content (TEC) variations during six geomagnetic storms of different intensity: from Dstmin = – 46 nT to Dstmin = -223 nT. The values of TEC deviations from its 27-day median value (δTEC) were calculated during the periods of the storms along three meridians: American, Euro-African and Asian-Australian. The following results were obtained. For the majority of the storms almost simultaneous occurrence of δTEC maximums was observed along all three meridians at the beginning of the storm. The transition from weak storm to superstorm (the increase of magnetic activity) almost does not affect the intensity of δTEC maximum. The seasonal effect was most pronounced at Asian-Australian meridian, less often at Euro-African meridian and was not revealed at American meridian. Sometimes the seasonal effect can penetrate to the opposite hemisphere. The character of averaged δTEC variations for the intense storms was confirmed by GOES satellite data. Though there are some common features of TEC variation revealed during each storm phase, in general no clear dependence of TEC responses on the storm phases was found: the effects were different during each storm at different locations. The behaviour of correlation coefficient (R) between δTEC at three meridians was analyzed for each storm. In general, R>0.5 between δTEC averaged along each meridian. This result is new. The possible reasons for the exceptions (when R < 0.5) were provided: time-shift of δTEC maximum at different latitudes along the American meridian, the complexity of phenomena during the intense storms and discordance in local time of geomagnetic storm beginning at different meridians. Notwithstanding the complex dependence of R on the intensity of magnetic disturbance, in general R decreased with the growth of storm intensity.

Keywords: ionospheric disturbances, magnetosphere-ionosphere interactions.

1 Introduction

The changes in the Earth's geomagnetic field provoked by Space Weather events can cause ionospheric disturbances. The last are very complex phenomena. One of the parameters that help to estimate the ionosphere state change is the vertical Total Electron Content (TEC) that is the quantity of electrons in a column of unit cross section (Davies and Hartmann, 1997; Afraimovich and Perevalova, 2006). Usually, TEC is calculated using phase and code delays of GNSS satellites signals received by dual frequency ground-receivers. The ionosphere is represented by a thin shell of zero thickness at the altitudes of the ionospheric F-region when calculating TEC (Shaer et al., 1995; Komjathy, 1997). Though TEC is an integral characteristics (Electron content from the satellite to the ground), it is assumed that it characterizes the state of F-region of the ionosphere. This is due to the fact that the main contribution to electron content is provided by the ionospheric F-region. In recent years, TEC has been widely used for ionosphere diagnostics for local regions and on a global scale due to availability of signals in all-time, all-weather conditions around the globe (Panda et al., 2014) and the large coverage of GNSS receivers worldwide in comparison to other ground-based instruments such as ionosonde networks, radars, etc. Despite a large number of publications dedicated to the disturbed ionospheric state, new data are still interesting to analyze. In the majority of works data of vertical ionospheric sounding and TEC are used together. However, at present, TEC acts as an independent parameter, in particular to estimate disturbances as, for example, in works (Jakowski et al., 2006; Gulyaeva and Stanislawska, 2008).

The choice of events for the analysis usually varies from several storms, for instance 15 cases during 2006-2007 (Cander and Ciraolo, 2010) or 217 events between 2001 and 2015 (Liu et al., 2017), to the detailed studies of a particular event, as in (Astafyeva et al., 2015). In the present work we study the global ionospheric responses to six geomagnetic storms using TEC data. The storms of different intensity (from weak to severe) were chosen within a short time interval (one-year period). The effects of the storms of different intensity on ionosphere were compared.

A number of works addressed global ionosphere variations during disturbances. One of the possible approaches is to study the behaviour of parameters along different meridians (Mansilla, 2011; Astafyeva et al., 2015). The majority of studies of latitudinal or longitudinal dependences of ionospheric responses are limited to some latitude-longitude region, although there are studies of global density distributions. For example, Zhao et al. (2007) suggested the presence of a longitudinal effect of the ionospheric storm caused by geomagnetic disturbance. Rajesh et al. (2016) showed using GIM that mid-latitude electron density enhancements exhibit significant longitudinal dependence. Longitudinal varieties of the ion total density in the equatorial and mid-low latitudinal topside ionosphere at four local times were studied by (Chen et al., 2015). Latitudinal variations between longitudes 40ºE and 100ºE in the Indian zone were addressed by Bhuyan et al. (2002). Nogueira et al. (2013) examined the four-peaked structure in the observed topside ion density and its manifestation as longitudinal structures in TEC over South America. Dmitriev et al. (2013) performed the longitudinal analysis of the day-side ionospheric storms within the region of equatorial ionization anomaly during recurrent geomagnetic storms. Longitudinal features of electron

density distributions were studied in (Klimenko et al., 2015; Klimenko et al., 2016) for minimum solar activity using modeling, GPS and satellite observations.

The present study addresses the global longitudinal TEC features not limited by one particular latitude-longitude zone. Three longitude sectors being rather far from each other were chosen for the analysis: along the American meridian (100ºW), along the Euro-African meridian (15ºE) and along the Asian-Australian meridian (115ºE). The effects were studied along these three longitudes within the latitude interval between 60ºN and 60ºS.

The storms considered in the present study were also the subject of several case studies mostly for some particular region. For example, Polekh et al. (2016) addressed the event of March 17, 2015; Astafyeva et al. (2016) studied ionosphere during June 22, 2015; Chashei et al. (2016) considered ionospheric effects during the storm on December 20, 2015, etc. In our case the focus is on global effects.

The aim of this work was to reveal the features of TEC variations during the particular geomagnetic storms along three meridians: American, Euro-African and Asian-Australian. The tasks were to: (1) obtain TEC variations along each meridian, (2) find if there is any correlation between these variations, (3) reveal if there is a peculiar character of TEC behaviour during the considered storms if compare to the quiet conditions and how this character depends on the intensity of disturbance and on the meridian itself.

2 Data used for the analysis

2.1 Parameters of magnetic storms

Six geomagnetic storms within one-year interval between March 2015 and March 2016 were chosen for the analysis. This period lays on the descending phase of solar activity cycle, not far from its maximum occurred in 2014. The majority of the storms occurred during the winter time in Northern Hemisphere (if categorize March as a winter month) and summer time in Southern Hemisphere. We have chosen the storms of different intensity. Figure 1 (left panels) illustrates Dst-index variations characterizing the disturbances. Vertical lines indicate main phase (MP), recovery phase (RP) and the end of the storm (Te). In some cases sudden storm commencements (SSC) are also indicated.

Table 1 provides the information about each event under analysis. The number assigned to each storm is given in the first column. The same numbers are used to label the panels of Figure 1 (between the left and right columns). The dates of disturbances are given in the second column of Table 1. The time moments of the beginning of the main phase of the storm are given in the third column. Minimal Dst-index values are given in the fourth column. Fifth column shows SYM-H index minimum values to provide the full picture of disturbance. Sixth column shows the time of the beginning of the recovery phase of each storm. The last seventh column presents the time moments of the end of the storm (Te). Here, “e” means end. Main and recovery phases were defined based on Dst variation. Te moment corresponded to the end of the storm when Dst value was about (-10 ÷-15) nT or before the next SSC. The geomagnetic storms are presented in Table 1 from the less intense (first line) to the most intense (sixth line) according to the Dst-index. Gonzalez et al. (1994) introduced storm

classification: intense storms are characterized by Dst ≤ - 100 nT, moderate storms - by – 100 nT ≤ Dst ≤ - 50 nT, weak storms - by -50 nT ≤ Dst ≤ - 30 nT. According to this classification, the storm #1 (14.12.2015) is weak, the storm #2 (06.03.2016) is moderate, the storms #3, #4, #5 and #6 are intense. The last storm (17.03.2015) is called a superstorm in literature because it was the most intense storm of solar cycle 24. Thus, all six considered storms are of different intensities.

2.2 TEC data

TEC values were obtained from Global Ionospheric Maps (GIM) produced by International GNSS Service (IGS). GIM TEC are independently computed by four Analysis Centers of the International GPS Service for Geodynamics (CODE, JPL, UPS, ESA) and then ranked and combined according to the corresponding weight by the International GNSS Service to produce the IGS global vertical TEC maps (Hernandez-Pajares et al., 2009). These final IGS maps were used for this study. TEC values were extracted from IONEX-files, freely available by following the link ftp://cddis.gsfc.nasa.gov/pub/gps/products/ionex. GIM provides the spatial resolution of 5º longitude and 2.5º latitude worldwide, thus, it is a useful tool for ionosphere diagnostics on a global scale.

For each observation point median TEC value was calculated on the basis of 27 previous days for every two hours of the day (UT). Thus, its own median value was obtained for each day every two hours. Furthermore, the deviation of TEC was calculated and plotted during each storm as well as six days before and six days after it following Eq. (1):

$$\delta\mathrm{TEC} = \frac{(\mathrm{TECobs} - \mathrm{TECmed27})}{\mathrm{TECmed27}} \times 100\% , \quad (1)$$

where TECobs is the observed value, TECmed27 is a median value calculated for the 27 days prior to the day of observation.

2.3 Satellite and geomagnetic data

Data from GOES weather satellites that circle the Earth in a geosynchronous orbit was used in the analysis (https://satdat.ngdc.noaa.gov/sem/goes/). The altitude of their orbit is about 35800 km. GOES-13 is positioned at 75ºW longitude and the equator monitoring North and South America and the Atlantic Ocean. GOES-15 is positioned at 135ºW longitude and the equator monitoring North America and the Pacific Ocean. The coverage by two satellites extends approximately from 20ºW longitude to 165ºE longitude. The instruments for near-Earth Space Weather monitoring are installed on board including magnetometer, X-ray sensor, high energy proton and alpha detector, and energetic particles sensor.

To estimate geomagnetic conditions, the Dst and SYM-H indices values were used. Both indices are the indicators of global Space Weather effects. Data is freely available by following the link http://wdc.kugi.kyoto-u.ac.jp. Wanliss and Showalter (2006) showed that SYM-H index can be used as a de facto high-resolution of Dst-index as they are quite similar to characterize the storms of different intensity. This similarity is also seen in Fig. 1 (right and left columns). We used Dst-index to define main and recovery phases of the storms: (a) for the illustrative purposes as Dst-curve is less rugged; (b) as we use classification of the intensity of the storms based on Dst-index (Section 2.1).

3 Discussion of results

3.1 Specific features of TEC variations during the considered storms

Variations of δTEC were the main source of information about the changes in the ionosphere. According to this data, the bursts of δTEC occurred at the beginning of magnetic disturbance. The duration of these bursts varied within several hours. The behaviour of δTEC along American, Euro-African and Asian-Australian meridians was studied with 10º step in latitude from 60ºN to 60ºS.

3.1.1 Weak δTEC variations

Sometimes manifestations of disturbance in TEC during geomagnetic storms were weak or absent within the latitude range of ±20º near the equator. Figure 2 provides the example for the storm of December 31, 2015 at the Euro-African sector. Here, for the economy of space the plots are shown with the 20º latitude step along the longitude. Days in Universal Time (UT) were laid off along the X-axis; additionally markings were laid every 2 hours (UT). To confirm this example the more detailed picture of TEC behavior is considered for the case of latitude 20ºN from Fig. 2. Fig. 3 (panel a) shows the values of the observed TEC (TECobs, green curve), its 27-day running median (TECmed27, red dotted curve) and standard deviation σ for TECobs (blue curve). Main and recovery phases (MP, RP) and the end of the storm (Te) are marked with the vertical lines. Median values serve as a quiet reference. It is seen that TEC observed during December 31, 2015 – January 02, 2016 (storm period) in general followed its quiet pattern (Fig. 3 panel a). The maximal TEC deviation from its quiet state reached -28%. Such deviation can be referred to day-to-day variability. In contrast, the different picture was observed for the same latitude 20ºN but at the American meridian. Fig. 3 (panel b) shows the results: the geomagnetic storm first caused the positive and then the negative TEC disturbance with the maximal TEC change of 67% from its quiet state. This particular example proves the presence of weak (almost absent) TEC disturbances within the latitudes ±20º at the particular sector.

3.1.2 Seasonal effect

The presence of seasonal effects in δTEC variations was revealed for the following cases.

(a) During the storm #2 (March 6th, 2016) the positive phase of disturbance was the dominant effect in δTEC variations during the night hours (UT) between March 6-7 along the Asian-Australian meridian from latitude 60ºN to latitude 0º. In contrast, at the same meridian from 10ºS to 60ºS the positive phase was followed by negative phase. In other words, during this storm the positive disturbance covered the latitudes of winter hemisphere, meanwhile summer hemisphere was characterised by positive disturbance followed by negative disturbance.

(b) Similar picture was observed along the same (Asian-Australian) meridian during the storm #4 (December 20th, 2015). However, though the general tendency of δTEC was similar along the whole meridian (increase of values followed by

decrease), in terms of phases the positive phase followed by decrease of values prevailed in Northern (winter) hemisphere from latitude 60ºN to 30ºN (Fig. 4, panel a). Further, from 20ºN to 60ºS, the δTEC increase followed by the clear negative phase was observed. Here, the "summer" effect penetrated into the "winter" hemisphere.

(c) During the same storm #4 along the Euro-African meridian from December 20th to December 22nd (0 UT) the disturbance showed the "positive-negative-positive" sequence of phases from 60ºN to 10ºN. Here, the second positive phase was much more intense and the whole disturbance within the interval 30ºN - 0º began earlier. The latitudes of Southern hemisphere 0º- 60ºS were covered by the negative phase during December 21st with preceding positive phase almost disappearing.

(d) During the storm #5 (June 23, 2015) along the Euro-African meridian the negative phase in the form of two bays was observed from 60ºN to 0º (Fig. 4 panel b). From 10ºS to 60ºS the disturbance had more complex character and included two or more positive phases. At the same time along the Asian-Australian meridian the negative phase was observed between 60ºN and 20ºN (Fig. 4 panel c). Starting from 10ºN positive phase (sometimes various peaks) was followed by negative phase. At that, the positive phase was in the form of a very intense burst (+ 180% and more) at latitudes between 20ºS and 60ºS. In this case, the "winter" effect penetrated into Northern Hemisphere from South.

To sum up, according to our data (cases (a)–(d)), the seasonal effect consists in general dominance of negative phase (decrease of TEC) in summer and positive phase (increase of TEC) in winter. This conclusion is in accordance with the case study (Kil et al., 2003). In the present study the effect was observed mostly over the Asian-Australian sector and no seasonal effect was registered over the American sector. Kil et al. (2003) addressed the case of magnetic storm of July 20th, 2000, using GIM and low-orbit satellite data. They revealed clear seasonal effects: a dominance of the negative ionospheric storm in the summer (northern) hemisphere and the pronounced positive ionospheric storm in the winter (southern) hemisphere. Kil et al. (2003) also found that the Northern "summer" negative phase penetrated into the Southern hemisphere. Our results also prove the possibility of penetrating of the seasonal effect to the opposite hemisphere. However, in our case both examples (b) and (d) showed such penetration from Southern to Northern Hemisphere: summer effects and winter effects respectively. Thus, we may conclude that it does not depend on the season itself or on the hemisphere.

The storm analyzed by (Kil et al., 2003) was very intense (Dstmin = -300nT). Our examples prove that the seasonal effect can be observed during the magnetic disturbance of less intensity (but still intense): -98 nT (a), -155 nT (b and c), -204 nT (d).

Here, we briefly mention that Zhao et al. (2007) also showed with GIM TEC that during magnetic disturbances a negative phase occurred with higher probability in the summer hemisphere, while a positive phase - in the winter hemisphere. According to these authors, negative phase was most prominent near geomagnetic poles and positive phase was far from polar regions. According to our data within the latitudes ±60°, the positive phase is very probable during the disturbances. At the same time it is not contradictory as each geomagnetic storm is a particular unique event.

To conclude, the seasonal effects had longitudinal dependence: observed mostly over the Asian-Australian sector, sometimes over Euro-African sector and no seasonal effect was registered over the American sector.

3.1.3 Global picture of δTEC variations at three meridians

Figure 5 shows the averaged δTEC behaviour. Each panel (a-f) represents the results for the particular storm: from the weakest (panel a) to the strongest (panel f). Storm dates are indicated below the panels. The time-interval on the X-axis is the interval between the storm beginning and Te (individual for each storm), according to Table 1. Each panel consists of three plots: upper plot represents variations in the American sector, middle plot – in Euro-African and the lower plot – in Asian-Australian sector. The curve on each plot represents δTEC values averaged along one meridian over the latitudes 60°N – 60°S with 10° step (δTECav). In other words, the final δTECav curve represents the average of 13 δTEC values from different latitudes. This averaging is possible because according to our data the tendency of increasing or decreasing of δTEC was the same at different latitudes along one meridian in most cases (without the regard to the phase). The specific cases are described above and also considered below.

First, it is seen that the maximal δTECav lays close to storms main phase beginning. Physically, it is explained by the fact that usually the drastic increase of particle flows from magnetosphere into ionosphere occurs at the beginning of each storm that, in turn, results in TEC disturbance. It is known, that during the development of disturbance the critical frequencies of ionosphere decrease lower than their initial quiet level (Blagoveshchensky, 2011). The same behaviour is observed in TEC: minimum of δTECav values is observed after the increase of δTECav, caused by the main phase of storm.

The main feature seen in the panels "a", "b", "e" is approximately the same time (UT) of δTECav maximum occurrence at all the latitudes along three meridians. In regard to panels "c" and "d", their results were discussed above. To add, the δTECav maximum took place at the same time at Asian-Australian and Euro-African meridians. For American meridian the peaks are shifted in time as it was mentioned before and the peaks themselves are more diffused if compare with Asia and Europe. Let us consider a more detailed picture of each panel of Fig. 5.

Panel (a) has the shortest disturbance duration due to the weakness of geomagnetic storm on December 14th, 2015. This weak intensity is the reason of the slow ionospheric response and the particle precipitation occur with a certain delay from storm beginning. At that, the moments of δTEC maximums coincide at three meridians. In panel (b) δTECav maximums were well-pronounced and coincided in time at three meridians during the moderate storm on March 6th, 2016. Panel (c) illustrates the results for the storm on December 31st, 2015. Time of δTECav maximums occurrence was the same only at Asian-Australian and Euro-African meridians. Panel (d) illustrates the picture similar to panel "c", but for the storm on December 20th, 2015. Panel (e) shows the results for the intense storm of June 23rd, 2015. It was the only storm among the six that occurred during the summer at Northern Hemisphere and during the winter in Southern Hemisphere. However, no specific details were revealed in comparison to other considered storms. Panel (f) shows the results for superstorm of March 17th, 2015. Though it is the most intense storm among the six, in general δTECav variations do not differ from the other storms: the increase of δTECav was followed by its decrease. However, the negative phase was more pronounced if compare with the weak positive phase.

To conclude, there is no dependence of δTECav maximums at three meridians on the intensity of magnetic activity. We recall that the intensity of storms grows from panel "a" to panel "f", but no increase in δTECav variations is detected.

3.1.4 Global picture of δTEC response to main and recovery phases of the storms.

The ionospheric responses to geomagnetic storms at different observation points have their peculiarities due to the differences in local hours, wind systems, electrical fields and other local effects. In addition, geomagnetic storms in different regions can manifest themselves differently. For instance, the exact moments of geomagnetic storm beginning and its intensity can vary. To estimate qualitatively the global effects of storm phases at different latitudes along three meridians we applied some generalization. First, we used Dst-index as a global measure of geomagnetic field change. Furthermore, as it was mentioned above, the tendencies of TEC increasing/decreasing in most cases were similar at different latitudes along each meridian, thus we can consider the average effects along the meridians. With regard to the phase of TEC disturbance, the picture was similar along each meridian in one hemisphere and sometimes in both hemispheres along the whole meridian. The example of such picture is given in Fig. 6.

The rapid main phase of storm #1 (Table 1) provoked TEC increase (beginning of the positive TEC disturbance) during 3 hours of its duration in both hemispheres at three meridians. The only exception was Euro-African meridian at Southern Hemisphere: TEC was already augmented before the main phase (Fig. 6 panel b). The maximum of TEC bursts at all latitudes and meridians occurred during the few hours after the beginning of the recovery phase. The negative phase followed TEC bursts during the second half of the recovery phase at Euro-African and Asian-Australian meridians in Southern Hemisphere. In Northern Hemisphere and at the American meridian in Southern Hemisphere TEC presented the second positive phase (less intense than the first maximum).

The storm #2 was characterized by rapid Dst decrease (Figure 1) and, consequently, by the short main phase (3 hours as in the previous case). The recovery phase lasted 20 hours. As it is known the ionospheric response to geomagnetic storm can be immediate or with a delay in hours and even days. The last is our case. The effects in the ionosphere were observed during the recovery phase, probably because of the short duration of the main phase. In Northern Hemisphere the positive TEC bursts occurred in the middle of the recovery phase along the whole American and Euro-African meridians as well as in Southern Hemisphere along Asian-Australian meridian with the following decrease of TEC. In Northern Hemisphere at Asian-Australian meridian TEC had more complex behaviour and mostly was increased during the whole period of the storm.

The peculiarities of the storm # 3 were already mentioned in Section 3.1.1 (weak δTEC variations within ±20º). Except this feature, in Southern Hemisphere the main phase of geomagnetic storm caused mostly the positive TEC disturbance and the recovery phase caused one or two negative TEC disturbances.

For the storm #4, it can be assumed that the recovery phase provoked one or two negative phases of TEC disturbance at Asian-Australian meridian. The effects in other sectors were rather different to generalize them.

The case of the storm #5 is more complicated as it developed at the already disturbed background: three SSC provoked by the interplanetary shocks (Astafyeva et al., 2017) of different intensities occurred during the considered interval: 16:46 UT on June 21st, 05:47 and 18:30 UT on June 22nd. An intense geomagnetic storm (storm #5) followed the last SSC with its main phase between June 22nd and June 23rd (Fig. 1). In general, along the American, Southern part of Euro-African and Asian-Australian meridians the positive TEC disturbance was observed during the main phase and the negative disturbance – during the recovery phase.

The superstorm #6 provoked complex effects at different observation points. Among the common features of TEC are the following. Along the American meridian the TEC burst was mostly caused during the main phase in Northern Hemisphere and it was shifted towards the recovery phase in Southern Hemisphere. TEC burst was observed during the main phase along other two meridians. Negative TEC disturbance was detected during the recovery phase at all observation points.

To sum up, the following common features were revealed. During the recovery phases of the weak and moderate storms (#1, #2) TEC reached its maximum globally. Though there are some similar features found, in general the intense storms #3 and #4 provoked rather complex TEC responses without dependence on the phase. During the recovery phases of the most intense storms #5 and #6 negative TEC bays were observed. These results are confirmed with averaged TEC behavior in Fig. 5. It should be mentioned that though some similarities in ionosphere variations during the particular phases of storms were revealed, the whole picture is rather complex.

3.2 Data of GOES-13 satellite

To compliment the analysis of Figure 5 and for better understanding of phenomena the results of measurements at GOES satellite were involved in this study. Its orbit in the near Earth space is at the altitude of 35800 km that is in the Earth's magnetosphere. Among the measurements performed at the satellite there were the intensity of X-rays, protons with energies from >1 to >100MeV, electrons with energies from >0.8 to >4 MeV.

GOES data was studied during the periods of all six geomagnetic storms (Fig.1). The particle flows of protons and electrons were registered for all considered storms. However, for storms #1 - #4 (Fig.1, Table 1) the intensity of these flows did not differed significantly from its undisturbed rate. Rather high levels of particle flows were observed only for storms #5 and #6. Even for Dst values of order of -150 nT (storm #4) the flows level was rather low and only for Dst being lower than -200 nT it was significant (intense storms #5 and #6 with Dst values being -204 nT and -223 nT respectively). Thus, it was impractical to consider satellite data for the first four storms #1 - #4. Figure 7 shows the flows variations for storms #5 and #6. The moments of storm beginnings (To) and storm ends (Te) are labeled with vertical lines for both storms. Figure 1 shows that the amplitudes and the shapes of Dst curves were close for both disturbances. It was of interest to compare the satellite measurements of high energy particles - protons and electrons. Protons variations (p) are plotted in the upper half of the plots of Fig. 7, electrons variations (e) – in the lower parts. The beginnings of the two storms were approximately at the

moment of maximal proton radiation and the beginning of minimal electron flows. Then, the decrease of proton flow occurred in the interval To-Te, but electron flows increased from its minimal to maximal values during the same time. In general, the proton and electron flows during magnetic storms are probably not directly connected with electron density in the ionosphere (Afraimovich and Perevalova, 2006). However, it is possible implicitly. The increase in δTECav values (Fig.5) at the beginning of the storm was probably related to the maximum of proton rates. The decrease in electron flux coincided with δTECav decrease. Further, the drastic growth of electron flux intensity took place leading to δTECav growth in Fig.5. In particular, for the storm #5 (June 23rd, 2015) Fig. 5 illustrates δTECav bursts before June 23rd, then the decrease to the minimum around June 24th and then again some increase between June 24th – 25th. Similar picture was observed during storm #6 (March 17th, 2015): the maximal intensity of the proton flux was accompanied with small δTECav increase (not significant in this case but existing) near the storm beginning (Fig.5,f) and then the decrease of the flux took place. During March 17th-18th the electron flux minimum was observed and then its increase. Thus, the character of δTECav behaviour for two storms in some way is proved by satellite data of energetic protons and electrons.

3.3 Similarities and differences of δTEC response at different meridians during the storms

We estimated a degree of correlation between δTECav at different meridians for each storm during the disturbed periods. This interval was different for each storm. Thus, 16 δTECav values were found within To-Te during storm #1; 23 values – during storm #2; 25 – during storm # 3; 49 - during storm # 4; 33 – during storm #5 and 58 – during storm #6. The distances in degrees between the meridians are the following: American – Euro-African (Am-E) – 115º, Euro-African – Asian-Australian (E-A) - 100º, Asian-Australian – American (A-Am) - 145º. The shortest distance is between E-A meridians and the largest – between A-Am meridians. Table 2 shows values of correlation coefficient (R) calculated between δTEC values at different meridians: (1) averaged at along the whole meridian (bold type), (2) averaged along the meridian in Northern Hemisphere (normal type), (3) averaged along the meridian in Southern Hemisphere (italic type).

3.3.1 δTEC averaged along the whole meridians

Table 2 illustrates the following features for averaging along the whole meridian (bold type).

- Rather high degree of correlation (R>0.5) took place between the δTEC variations during storms #1-#5 for all meridians except two values R = 0.148 and R = 0.430 between Asian-Australian and American meridians. This is explained by the time shift of δTEC peak along the American meridian as shown in Fig.5 (panels c and d). We associate low correlations during storm #6 with the complexness of local phenomena because of the high intensity of the storm (including no correlation in the case A-Am).

- The highest R values (if comparing three pairs of meridians) were found between European and Asian-Australian sectors in five cases of six.

- The highest R values between all three meridians (R>0.5) were during the weakest storm #1. This corresponds to the physics of phenomena. Perturbations and irregularities in the ionosphere are more pronounced during intense

disturbances than during moderate or weak disturbances. During the weak storm the ionosphere structure is not significantly changed and its global stability is retained.

- The lowest R values (in bold) took place between Asian-Australian and American sectors if compare to other two pairs at least for five storms of six. It is probably explained by the fact that the distance between the American and Asian meridians is the largest (145º). Another possible cause is that storm beginnings were observed in the contrary local time zones (day or night local hours) for these two meridians during all storms under analysis.

- The not evident, mixed dependence of R on the intensity of magnetic disturbance is common for all three meridians. For example, the comparison of R for storms #1 - #4 shows that R are decreasing from values R = 0.884 (Am-E), R = 0.815 (E-A), R = 0.744 (A-Am) to values R = 0.522 (Am-E), R = 0.615 (E-A), R = 0.430 (A-Am) during disturbances. This is in accordance with physics of phenomena. However, the transition from the storm #4 to the storm #6 shows inverse dependence: some growth of R instead of its decrease for storm #5. Nevertheless, in general, R behaviour in dependence to the intensity of magnetic disturbance (transition from storm #1 to storm #6) showed the decrease of R values, which is to be expected. The lowest R values were for the most intense storm.

3.3.2 δTEC averaged along meridians in each hemisphere

It is known that TEC behavour has a seasonal dependence (Afraimovich and Perevalova, 2006). As the seasons are opposites in two hemispheres, the effects in North and South can be different. In general, it is revealed that the intense bursts of δTEC took place at subpolar latitudes of both hemispheres. To compare "northern" and "southern" data first the averaging of δTEC was performed along each meridian separately in each hemisphere: between the latitudes 60ºN-10ºN (northern) and then between the latitudes 10ºS – 60ºS (southern). Middle and lower panels of Fig. 6 serve the example. Though the averaging along the meridian implies only qualitative, not quantitative estimate of deviations, it was of interest to analyze the effects separately. Table 2 presents the results of R calculations made separately for Northern (normal type) and Southern (italic type) hemispheres.

- For two storms #5 and #6 close by their intensities of disturbance, but different by the season of occurrence (summer/winter and winter/summer) the following is characteristic. R<0.5 in Northern hemisphere (summer) and R>0.5 in Southern hemisphere (winter) at all three meridians during the storm #5. For the storm #6 the opposite picture is seen. R<0.5 in both hemispheres and there was no correlation in cases Am-E and A-Am. But in cases of correlation existence, R was lower in Southern hemisphere (summer) than in Northern hemisphere (winter) when the correlation was detected (E-A). It may be related to the seasonal effect, but more statistics is needed to conclude.

- Comparison of R for Southern and Northern hemispheres shows rather high degree of correlation in both hemispheres simultaneously (R>0.5) only for the weak storm #1. For other storms the number of cases when R<0.5 increases with the disturbance intensity: one case for the storm #2, two cases for the storm #3, three cases for storms #4 and #5, five cases for storm #6. In other words, the difference in R values in Northern and Southern hemispheres grows with the increase of magnetic activity. It results that seasonal effect has impact here.

- The correlation coefficients, R, calculated along a whole meridian (bold values) are close to maximal R values either of Northern or Southern hemisphere.

3.3.3 δTEC at three meridians in each latitude sector (without averaging)

We briefly mention that R behaviour was also studied without averaging (at each latitude separately). The results confirmed the last conclusion of issue 3.3.1: the lower the intensity of magnetic storm, the more the number of moderate and strong correlations between δTEC at different latitudes (R>0.45). Mild and weak correlations prevailed with the growth of the intensity of storms. The number of negative correlations also increased with the storm intensity growth. For instance, 11 such cases of total 39 were found for the superstorm #6.

For storm # 5 (June 23, 2015) R behaviour was found to be similar for all three pairs of meridians: R was positive within the latitudes ±60º and ±10º (in both hemispheres) and R was rather low or negative within the interval from 10Nº to 10Sº. Consequently, the ionosphere processes in equatorial zone were due to different physical causes at three meridians.

3.4 Conclusions

The features of behaviour of Total Electron Content deviation from its 27-day median value were studied during six geomagnetic storms of different intensity along three meridians: American, Euro-African and Asian-Australian. The storms were chosen within a short period of time (one year). Though six storms is not a big statistics, some features of TEC variations during these particular events were obtained.

1) During the majority of considered storms at all meridians the maximum of δTEC bursts occurred almost simultaneously at high latitudes in North and South and at the equator provided that the consideration was along each meridian separately. The analysis of TEC response to each storm phase separately showed rather complex picture. The following common features were revealed. During the recovery phases of the weak and moderate storms TEC reached its maximum globally. During the recovery phases of the most intense storms (Dst <-200 nT) negative TEC bays were observed. During other two intense storms (Dst > -200 nT), no clear dependence of TEC responses on the storm phases was found.

2) It was revealed that the beginning of TEC disturbance during the superstorm March 17, 2015, qualitatively did not differ from the beginning of other storms: increase of δTECav was followed by its decrease. The transition from weak storm to superstorm (the increase of magnetic activity) almost does not influence the intensity of δTECav maximum.

3) The seasonal effect (general dominance of negative/ positive phase in summer/winter) was observed mostly at Asian-Australian meridian. No seasonal effect was registered over American sector. Our results prove the possibility of the seasonal effect penetrating to the opposite hemisphere (in our case from the Southern to Northern Hemisphere). We did not found out dependence of such penetrations on the season itself or on the hemisphere.

4) The character of δTEC for most intense storms under analysis (June 23rd, 2015 with Dstmin = -204 nT and March 17th, 2015 with Dstmin - -223 nT) is rather similar despite of the opposite seasons of occurrence of storms and in some way is confirmed by GOES satellite data of energetic proton and electron fluxes.

5) The analysis of correlation coefficients between averaged δTEC variations at three meridians during each storm showed the following.

- The degree of correlation between averaged along a whole meridian δTEC values at three meridians was rather high (R>0.5). This result is new. There are five exceptions of 18 cases from Table 2: (a) R = 0,148 and R = 0.430, both found between Asian-Australian and American meridians, and (b) low R during the most intense storm #6. Issue (a) is related to the time-shift of δTEC maximum at different latitudes along the American meridian. The reason of the shift is provided. Issue (b) is associated with the complexity of phenomena during the most intense storm.

- The highest coefficients of correlation between averaged along a whole meridian δTEC (all three R>0.5) took place during the weakest storm. This is due to the fact that during the weak storm the ionosphere structure is not significantly changed and its global stability is retained. Comparison of R between δTEC averaged separately in Northern and Southern hemispheres also showed that high degree of correlation for both hemispheres R>0.5 took place only for the weak storm. The difference between hemispheres increased with the increase of magnetic activity, that probably again is explained by seasonal effect.

- The lowest coefficients of correlation (through all the storms in general) were found between Asian-Australian and American meridians. The reasons may include the largest distance between these meridians and discordance in local time of storm occurrence.

- The not evident, mixed dependence of R on the intensity of magnetic disturbance is common for all three meridians. Nonetheless, the transition from weak to the most intense storm shows the decrease of correlation till the absence or even negative correlations. This result is new. It is confirmed by correlation coefficients between both averaged δTEC and δTEC at each latitude separately. In general, the more the intensity of magnetic disturbance, the lower the correlation rates between δTEC variations at three meridians.

- Calculation of R separately for two hemispheres allowed us to reveal that the most intense δTEC bursts took place at subpolar latitudes of both hemispheres. For two storms 23.06.2015 and 17.03.2015 close by the intensity but different by the season the following is revealed. For summer storm 23.06.2015 R values were less than 0.5 in Northern hemisphere and more than 0.5 – in Southern hemisphere between all three meridians. For storm 17.03.2015 R values were less than 0.5, but in general, the picture was vice versa: correlation coefficients were lower in Southern hemisphere and higher – in Northern (when correlation was detected). The seasonal effect probably plays a main role here.

- For the storm of June 23, 2015, R between δTEC at each latitude for all three pairs of meridians was positive within the latitudes ±60º and ±10º (in both hemispheres) and was rather low or negative within the interval 10Nº-10Sº. Consequently, the ionosphere processes in equatorial zone were the subject of different physical causes at three meridians.

3.5 Acknowledgments

The work was supported by grant № 18-05-00343 from Russian Foundation for Basic Research. The work of Maltseva O.A. was supported by grant under the state task N3.9696.2017/8.9 from Ministry of Education and Science of Russia. SCiESMEX is partially funded by CONACyT-AEM Grant 2014- 01-247722, CONACyT LN 269195, and DGAPA-PAPIIT Grant IN106916. M. Sergeeva acknowledges the partial funding by the Sectoral Fund for Research, Technological Development and Innovation in Space Activities, CONACYT-AEM (project 292700, 28/05/2018).

The authors express their gratitude to the services of IGS for the opportunity to use IONEX data via Internet. We also thank NOAA's National Centers for Environmental Information for the opportunity to use GOES satellite data (https://satdat.ngdc.noaa.gov). Dst and SYM-H indices data was obtained from Data Analysis Center for Geomagnetism and Space Magnetism, Kyoto University (http://wdc.kugi.kyoto-u.ac.jp).

The authors would like to thank the anonymous reviewers for their contributing comments.

References

Afraimovich, E.L. and Perevalova N.P.: GPS-monitoring of Earth upper atmosphere. Irkutsk, Russian Academy of Sciences, Siberian Branch, 460p. ISBN 5-98277-033-7, 2006.

Astafyeva, E., Zakharenkova, I. and Alken, P.: Prompt penetration electric fields and the extreme topside ionospheric response to the June 22–23, 2015 geomagnetic storm as seen by the Swarm constellation. Earth, Planets and Space, 68:152, doi: 10.1186/s40623-016-0526-x, 2016.

Astafyeva, E., Zakharenkova, I. and Forster, M.: Ionospheric response to the 2015 St. Patrick's Day storm: a global multi-instrumental overview. J. Geophys. Res. Space Phys. 120, 9023–9037, doi: 10.1002/2015JA021629, 2015.

Bhuyana, P.K., Chamuaa, M., Bhuyana, K., Subrahmanyamb, P. and Garg, S.C.: Diurnal, seasonal and latitudinal variation of electron density in the topside F-region of the Indian zone ionosphere at solar minimum and comparison with the IRI. Journal of Atmospheric and Solar-Terrestrial Physics, 65 359–368, doi: 10.1016/S1364-6826(02)00294-8, 2003.

Blagoveshchensky, D.V.: Short waves in the anomalous radio channels. Saarbrücken, Germany, LAP LAMBERT Academic Publishing GmbH&Co. KG, 422p, 2011.

Blagoveshchensky, D.V., Pirog, O.M., Polekh, N.M. and Chistyakova, L.V.: Mid-latitude effects of the May 15, 1997 magnetic storm. Journal of Atmospheric and Solar-Terrestrial Physics, 65, 203–210, 2003.

Cander, Lj.R. and Ciraolo, L.: Ionospheric Total Electron Content and Critical Frequencies over Europe at Solar Minimum. Acta Geophysica, 58(3), 468-490, doi: 10.2478/s11600-009-0061-2, 2010.

Chashei, I.V., Tyul'bashev, S.A., Shishov, V.I. and Subaev, I.A.: Interplanetary and ionosphere scintillation produced by ICME. Space Weather, 14, 682–688, doi: 10.1002/2016SW001455, 2016.

Chen, Y.N. and Xu, J.S.: Longitudinal structure of plasma density and its variations with season, solar activity and dip in the topside ionosphere. Chinese Journal of Geophysics, 58(6), 1843-1852, doi: 10.6038/cjg20150601, 2015.

Danilov, A.D.: Ionospheric F-region response to geomagnetic disturbances. Advances in Space Research, 53(3), 343-366, 10.1016/j.asr.2013.04.019, 2013.

Davies, K. and Hartmann, G.K.: Studying the ionosphere with the Global Positioning System. Radio Science, 32(4), 1695-1703, doi: 10.1029/97RS00451, 1997.

Dmitriev, A.V., Huang, C.-M., Brahmanandam, P.S., Chang, L.C., Chen, K.-T. and Tsai, L.-C.: Longitudinal variations of positive dayside ionospheric storms related to recurrent geomagnetic storms. J. Geophys. Res. Space Physics, 118, 6806-6822, doi : 10.1002/igra.50575, 2013.

Gonzalez, W.D., Joselyn, J.A., Kamide, D., Kroehl, H.W., Rostoker, G., Tsurutani, B.T. and Vasyliunas, P.: What is a geomagnetic storm? J. Geophys. Res., 99(A4), 5771-5792, 1994.

Gulyaeva, T.L. and Stanislawska, I.: Derivation of a planetary ionospheric storm index. Ann. Geophys., 26, 2645–2648, 2008.

Jakowski, N., Stankov, S.M., Schlueter, S. and Klaehn, D.: On developing a new ionospheric perturbation index for space weather operations. Adv. Space Res., 38, 2596-2600, 2006.

Kil, H., Paxton, L.J., Pi, X., Hairston, M.R. and Zhang, Y.: Case study of the 15 July 2000 magnetic storm effects on the ionosphere-driver of the positive ionospheric storm in the winter hemisphere. Journal of Geophysical Research, 108(A11), 1391, doi: 10.1029/2002JA009782, 2003.

Klimenko, M.V., Klimenko, V.V., Bessarab, F.S., Zakharenkova, I.E., Vesnin, A.M., Ratovsky, K.G., Galkin, I.A., Chernyak, Iu.V., Yasyukevich, Yu.V., Koren'kova, N.A. and Kotova, D.S.: Diurnal and Longitudinal Variations in the Earth's Ionosphere in the Period of Solstice in Conditions of a Deep Minimum of Solar Activity. Cosmic Research, 54(1), 8–19. doi: 10.1134/S001095251601010X, 2016.

Klimenko, M.V., Klimenko, V.V., Zakharenkova, I.E., Vesnin, A.M., Cherniak, I.V. and Galkin, I.A.: Longitudinal variation in the ionosphere-plasmasphere system at the minimum of solar and geomagnetic activity: Investigation of temporal and latitudinal dependences, Radio Sci., 51, 1864–1875, doi: 10.1002/2015RS005900, 2016.

Komjathy, A.: Global ionospheric total electron content mapping using the Global Positioning System. Ph.D. Dissertation, Department of Geodesy and Geomatics Engineering Technical Report No. 188, University of New Brunswick, Fredericton, New Brunswick, Canada, 1997.

Liu, W., Xu, L., Xiong, C. and Xu, J.: The ionospheric storms in the American sector and their longitudinal dependence at the northern middle latitudes. Advances in Space Research, 59, 603–613, doi: 10.1016/j.asr.2016.10.032, 2017.

Luan, X., Wang, W., Dou, X., Burns, A. and Yue, X.: Longitudinal variations of the nighttime E layer electron density in the auroral zone. J. Geophys. Res. Space Physics, 120, 825–833, doi: 10.1002/2014JA020610, 2015.

Mansilla, G.A.: Moderate geomagnetic storms and their ionospheric effects at middle and low latitudes. Adv. Space Res., 48, 478–487, doi: 10.1016/j.asr.2011.03.034, 2011.

Nogueira, P.A.B., Abdu, M.A., Souza, J.R., Bailey, G J., Batista, I.S., Shume, E.B. and Denardini, C.M.: Longitudinal variation in Global Navigation Satellite Systems TEC and topside ion density over South American sector associated with the four-peaked wave structures. J. Geophys. Res. Space Physics, 118, 7940-7953, doi: 10.1002/2013JA019266, 2013.

Panda, S.K., Gedam, S. and Rajaram, G.: Study of Ionospheric TEC from GPS observations and comparisons with IRI and SPIM model predictions in the low latitude anomaly Indian subcontinental region. Advances in Space Research, 55, 1948-1964, doi: 10.1016/j.asr.2014.09.004, 2015.

Polekh, N.M., Zolotukhina, N.A., Romanova, E.B., Ponomarchuk, S.N., Kurkin, V.I. and Podlesnyi, A.V.: Ionospheric effects of magnetospheric and thermospheric disturbances on March 17-19, 2015. Geomagnetism and Aeronomy, 56(5), 557-571, doi: 10.1134/S0016793216040174, 2016.

Rajesh, P.K., Liu, J.Y., Balan, N., Lin, C.H., Sun, Y.Y. and Pulinets, S.A.: Morphology of midlatitude electron density enhancement using total electron content measurements. Journal of Geophysical Research: Space Physics, 1503-1507, doi: 10.1002/2015JA022251, 2016.

Schaer, S., Beutler, G., Mervart, L., Rothacher, M. and Wild, U.: Global and regional ionosphere models using the GPS double difference phase observable. Proceedings of the IGS Workshop, Potsdam, Germany, May 15-17,1995, 1-16, 1995.

Wanliss, J.A. and Showalter, K.M.: High-resolution global storm index: Dst versus SYM-H, Journal of Geophysical Research, 111, A02202, doi:10.1029/2005JA011034, 2006.

Zhao, B., Wan, W., Liu, L. and Mao, T.: Morphology in the total electron content under geomagnetic disturbed conditions: results from global ionosphere maps. Ann. Geophys., 25, 1555–1568, doi: 10.5194/angeo-25-1555-2007, 2007.

Table 1. Characteristics of the geomagnetic storms used in the analysis.

#	Date of storm beginning	Beginning of the main phase (based on Dst-index)	Minimum value of Dst-index	Minimum value of SYM-H index	Beginning of the recovery phase (based on Dst-index)	Te (storm end based on Dst-index)
1	14.12.15	16 UT, 14.12.15	-47 nT	-60 nT	19 UT, 14.12.15	22 UT, 15.12.15
2	06.03.16	16 UT, 06.03.16	-98 nT	-110 nT	21 UT, 06.03.16	12 UT, 08.03.16
3	31.12.15	12 UT, 31.12.15	-110 nT	-117 nT	00 UT, 01.01.16	12 UT, 02.01.16
4	20.12.15	03 UT, 20.12.15	-155 nT	-170 nT	22 UT, 20.12.15	23 UT, 23.12.15
5	22.06.15	17 UT, 22.06.15	-204 nT	-208 nT	04 UT, 23.06.15	05 UT, 25.06.15
6	17.03.15	07 UT, 17.03.15	-223 nT	-234 nT	22 UT, 17.03.15	17 UT, 21.03.15

Table 2. Correlation coefficients between δTEC at three meridians.

#	Date of storm	American - Euro-African (Am-E)	Euro-African - Asian-Australian (E-A)	Asian-Australian - American (A-Am)
1	14.12.15	**0.884** 0.745 *0.561*	**0.815** 0.857 *0.640*	**0.744** 0.621 *0.744*
2	06. 03.16	**0.737** 0.746 *0.635*	**0.689** 0.298 *0.673*	**0.791** 0.577 *0.758*
3	31.12.15	**0.644** 0.685 *0.394*	**0.791** 0.738 *0.808*	**0.148** 0.574 *0.012*
4	20.12.15	**0.522** 0.556 *0.239*	**0.615** 0.499 *0.508*	**0.430** 0.729 *0.128*
5	23.06.15	**0.672** 0.449 *0.717*	**0.832** 0.158 *0.854*	**0.724** 0.467 *0.716*
6	17.03.15	**0.362** 0.279 *0.071*	**0.463** 0.172 *0.509*	**0.004** 0.332 *-0.086*

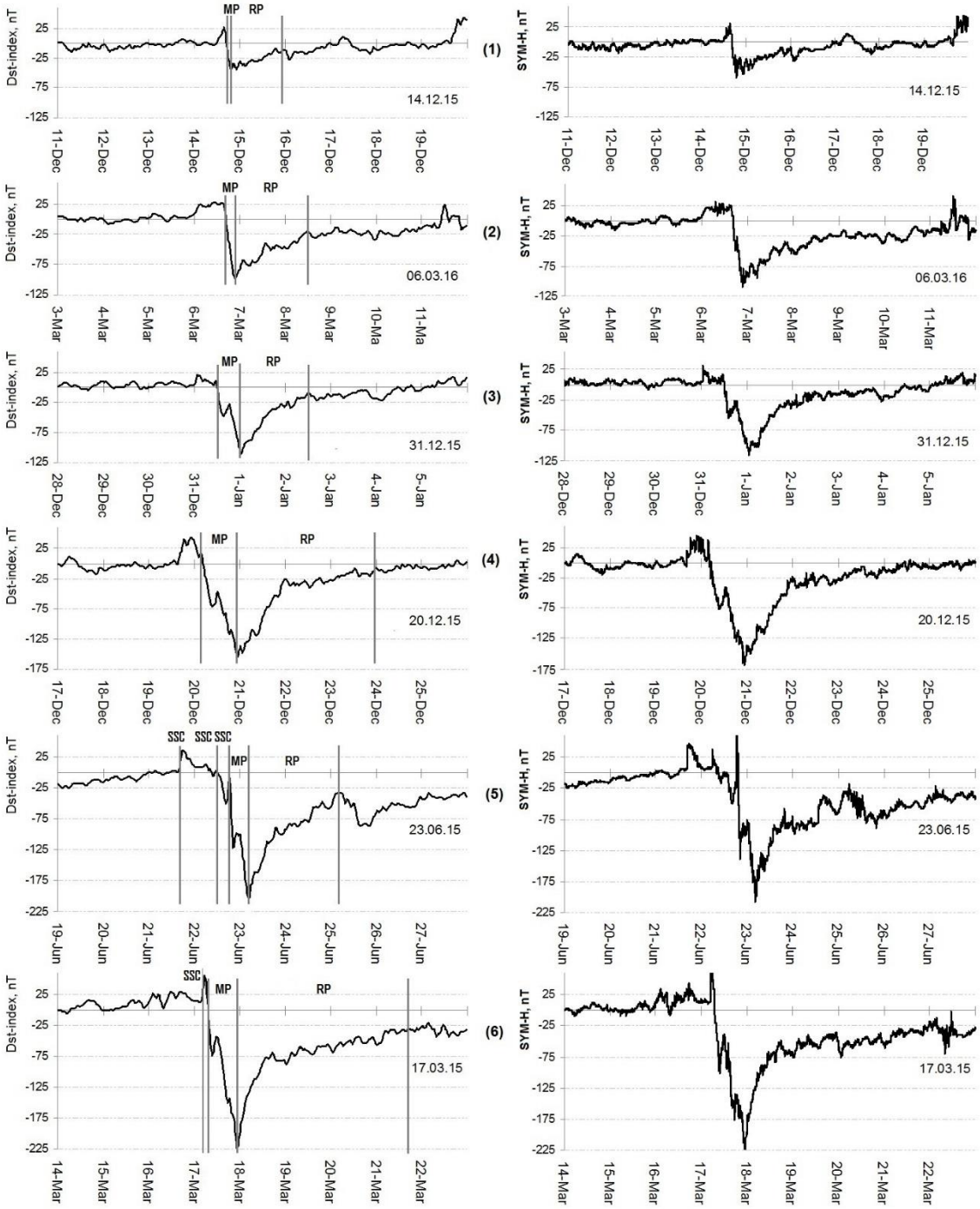

Figure 1: Dst-index (left column) and SYM-H index (right column) variations during the periods of six geomagnetic storms under analysis. Main (MP) and recovery phases (RP) as well as sudden storm commencement (SSC) were marked by vertical lines based on Dst-index variation.

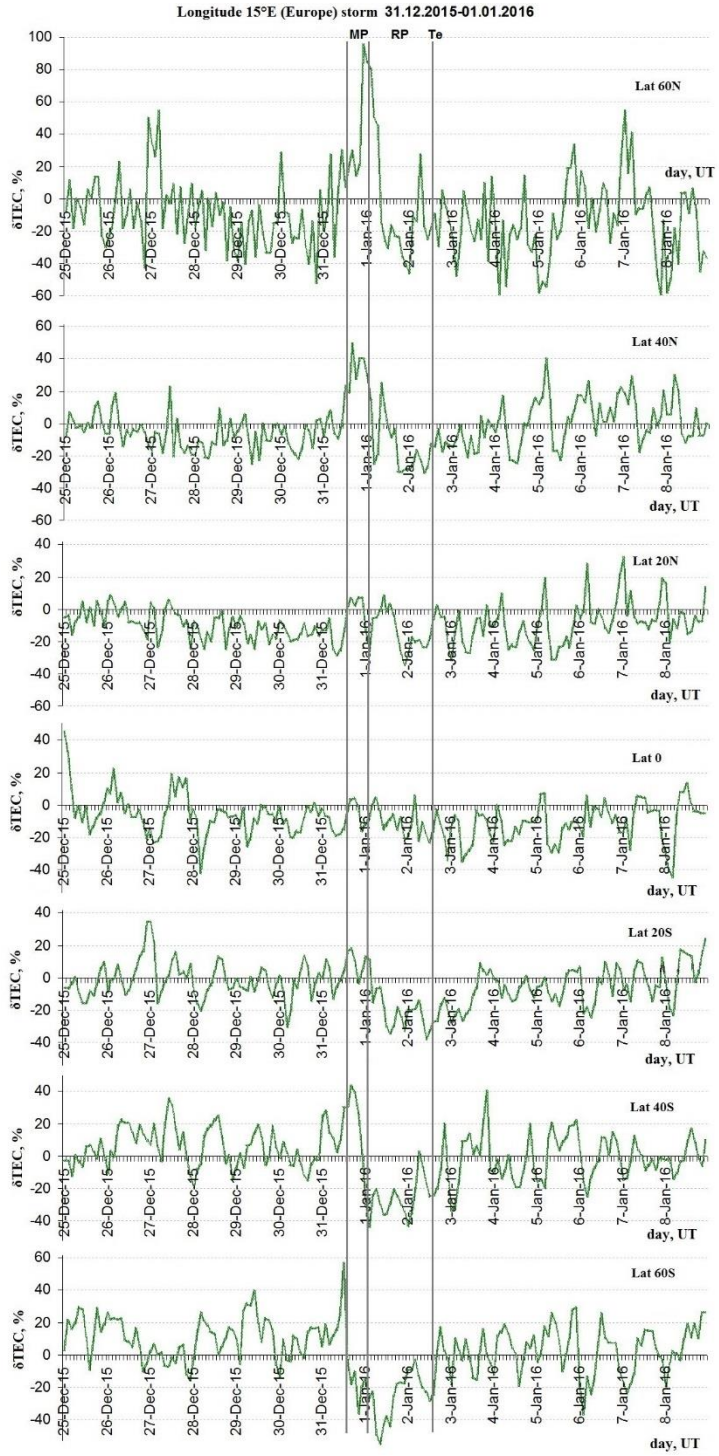

Figure 2: Weak manifestation of TEC effects within the latitudes ±20º during the storm of December 31st, 2015. MP, RP and Te are marked with vertical lines.

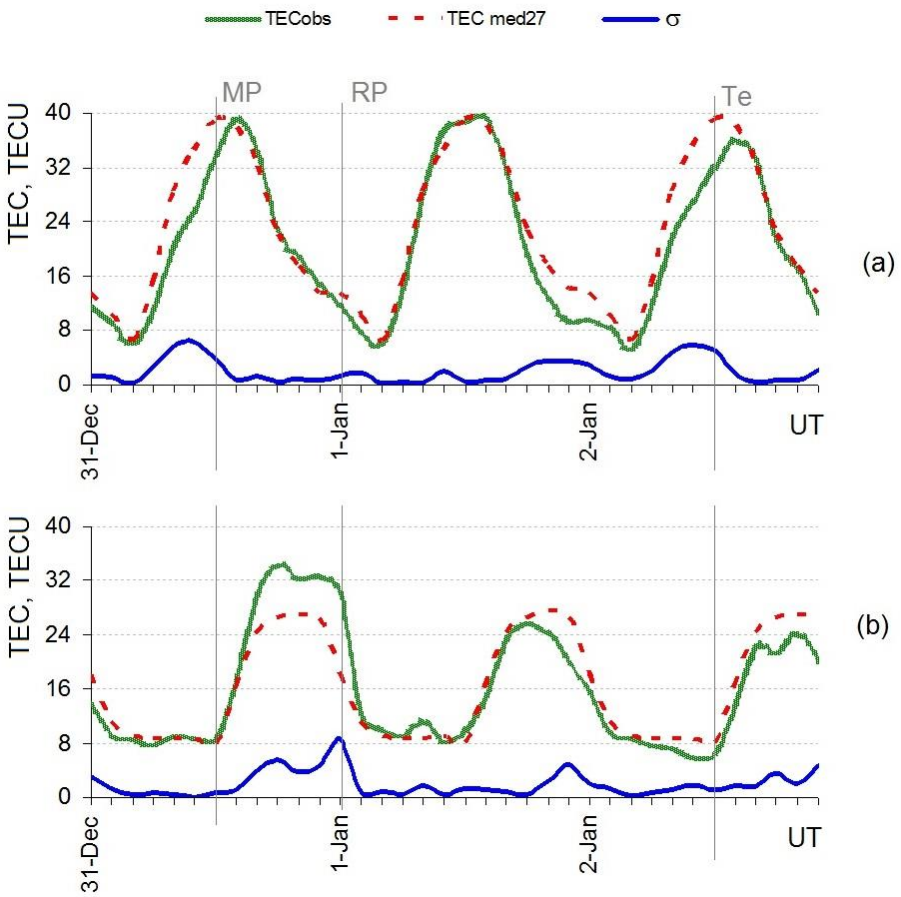

Figure 3: Results for storm #3 at latitude 20ºN: for Euro-African (panel a) and American meridian (panel b). Observed TEC (green curve), 27-day running median (red dotted curve) and standard deviation σ for the observed TEC (blue curve). MP, RP and Te are marked with vertical lines.

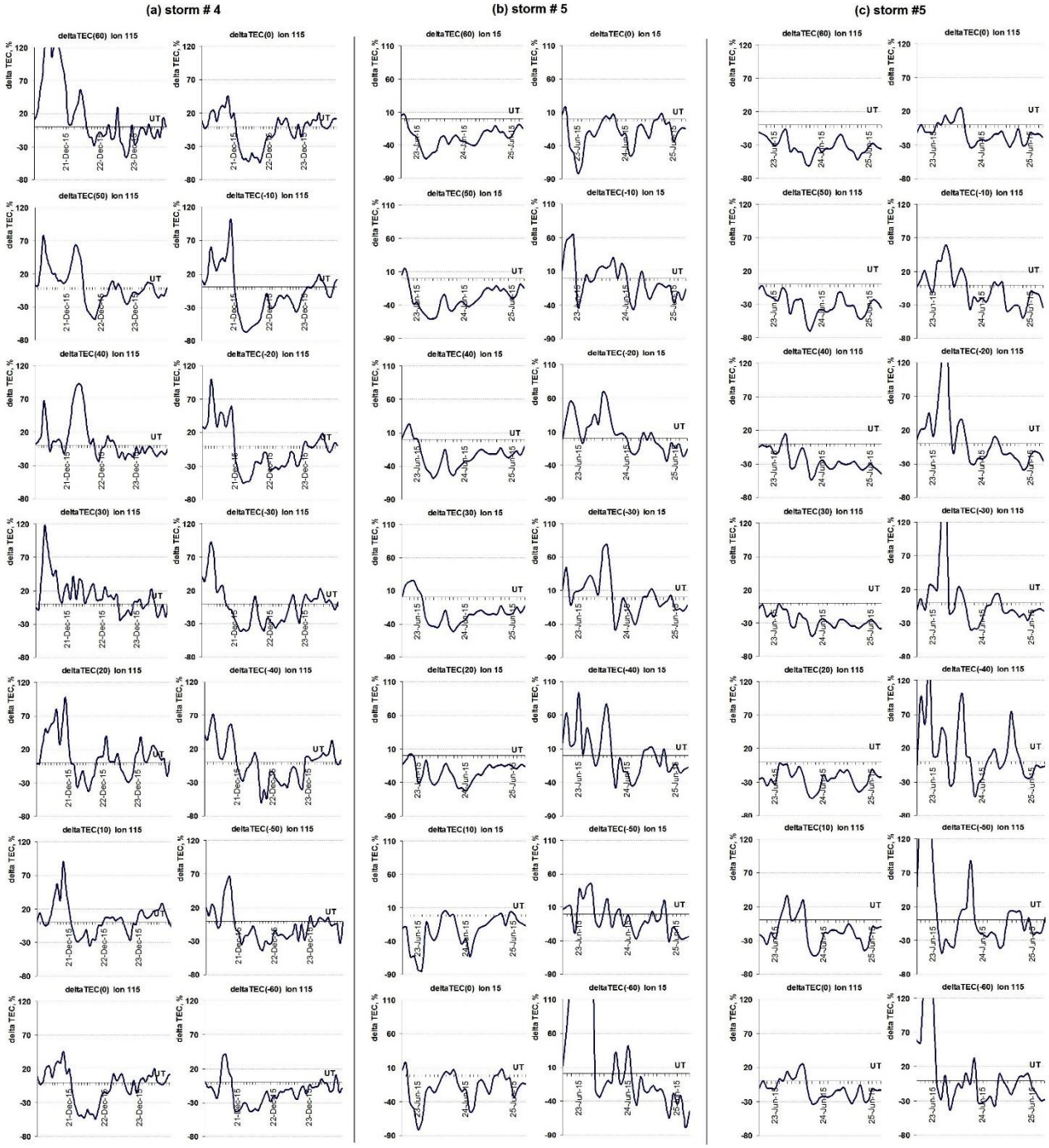

Figure 4: δTEC variations for storms: (a) #4 at Asian-Australian meridian; (b) #5 at Euro-African meridian; (c) #5 at Asian-Australian meridian. Left plots of each panel display variations in the Northern and right plots– in the Southern Hemispheres.

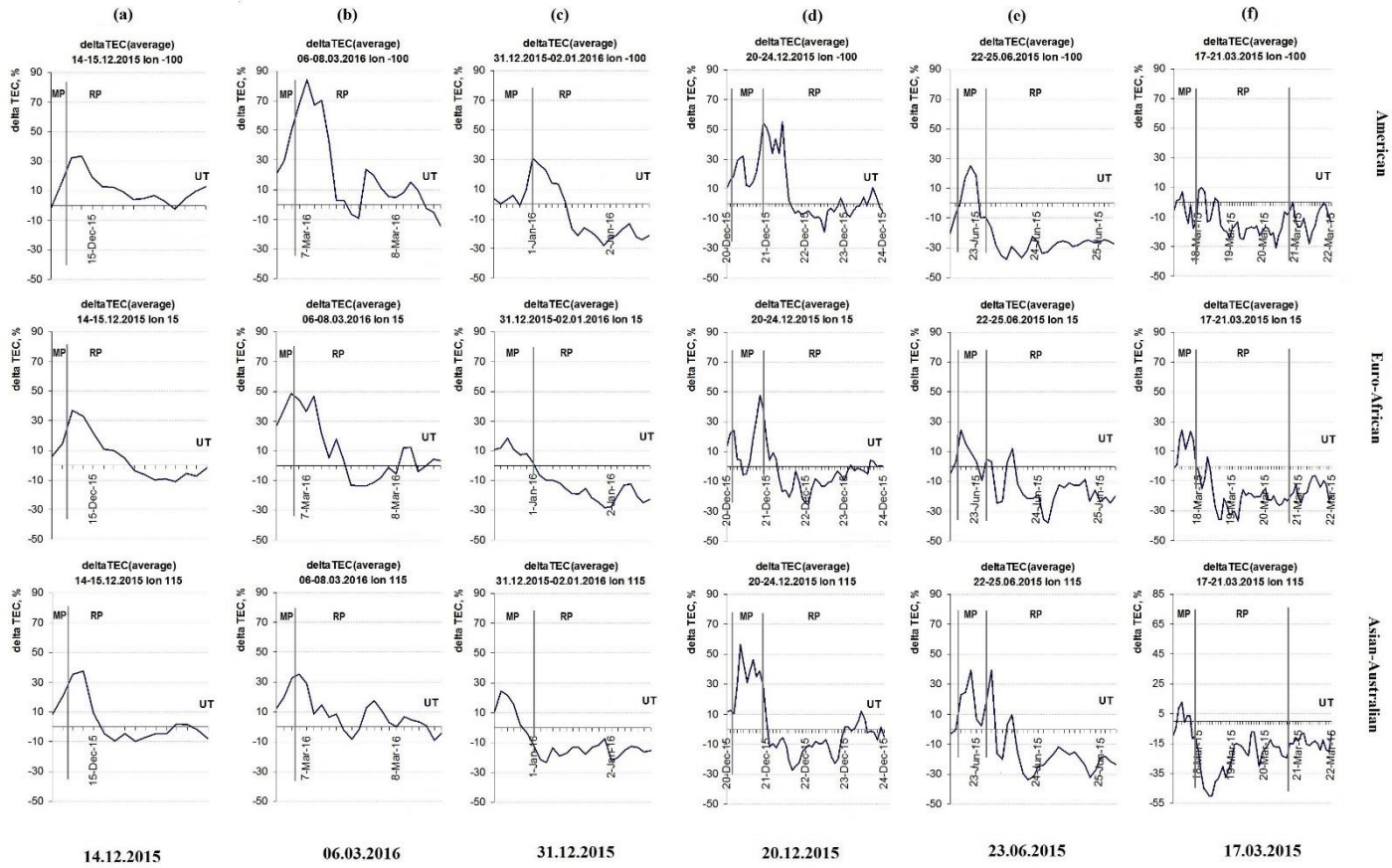

Figure 5: δTEC averaged along each meridian during the storms. Vertical lines indicate the periods of MP and RP.

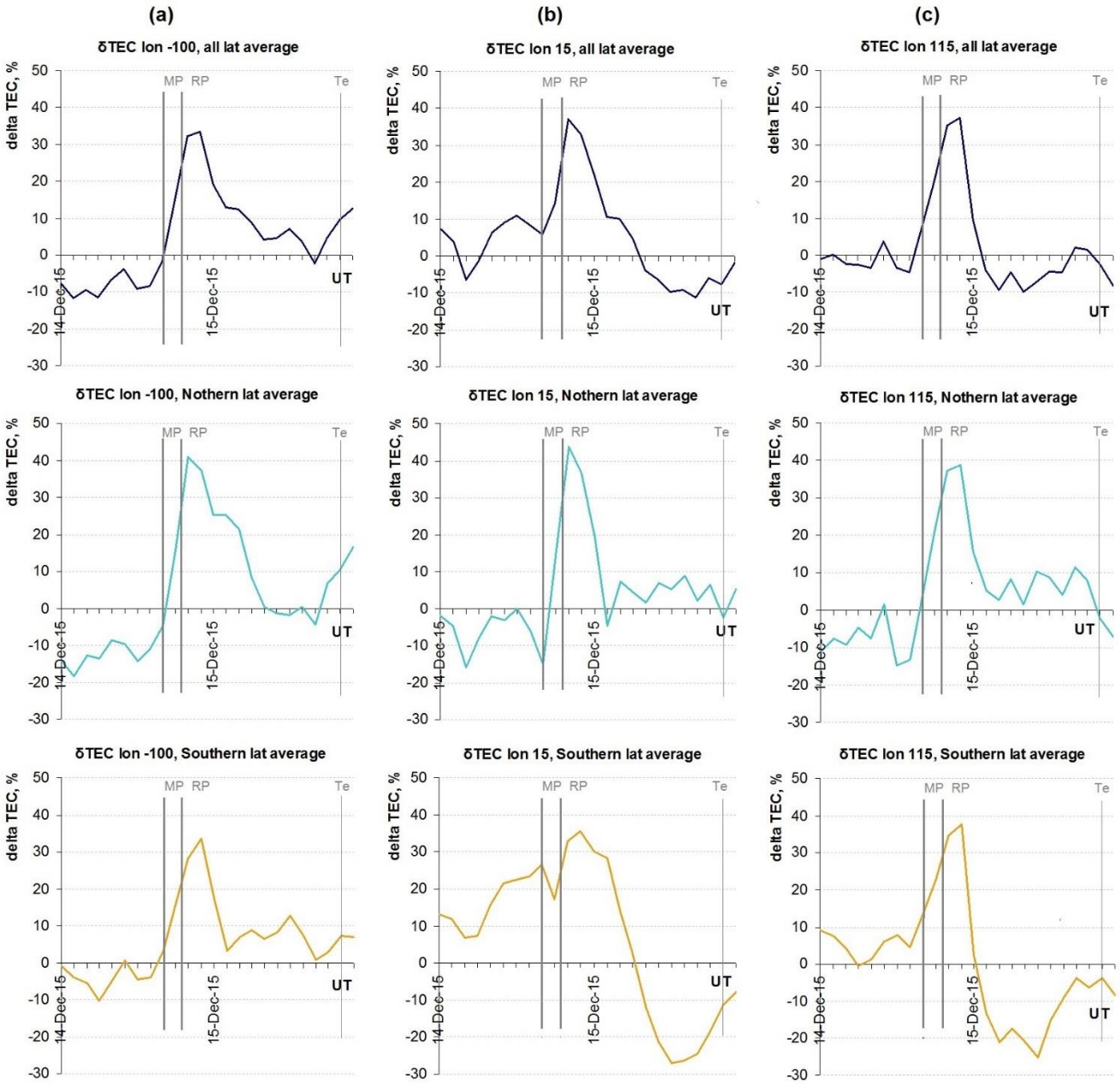

Figure 6: Results for storm #1: δTEC averaged along the whole meridian (upper panels), along the Northern hemisphere latitudes (middle panels) and along the Southern Hemisphere latitudes (lower panels) at the American (column a), Euro-African (column b) and Asian-Australian (column c) meridians. MP and RP beginnings and Te are marked by vertical lines.

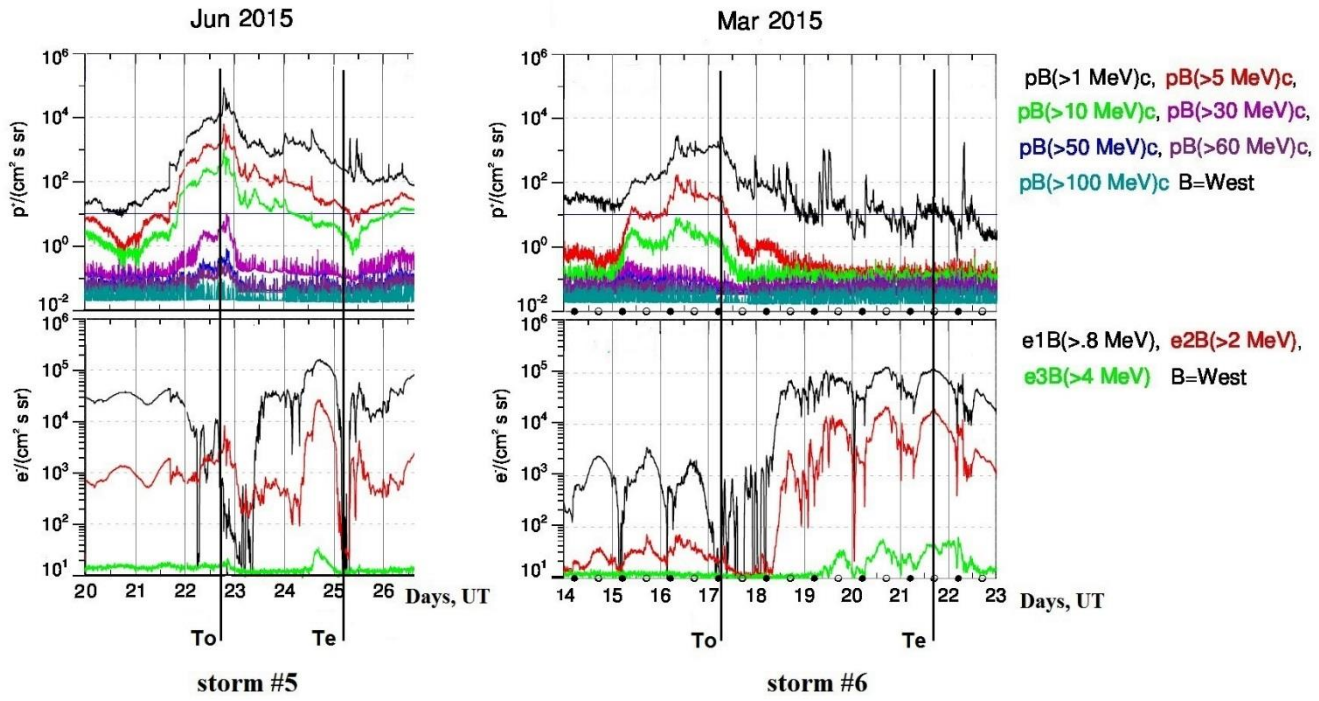

Figure 7: GOES satellite data for storms #5 and #6: p – protons, e – electrons. The particle energy is labeled by colors. The beginning (To) and the end of the storm (Te) are marked with vertical lines.